Crystalline Structure of Some Poly(ferrocenylenedialkylsilylenes)

V. S. Papkov,* M. V. Gerasimov, and I. I. Dubovik

Nesmejanov Institute of Organoelement Compounds, Russian Academy of Sciences, Vavilov str., 28, 117813 Moscow, Russia

S. Sharma, V. V. Dementiev, and K. H. Pannell*

Department of Chemistry, University of Texas at El Paso, El Paso, Texas 79968

Received February 25, 2000; Revised Manuscript Received June 23, 2000

ABSTRACT: X-ray diffraction studies on poly(ferrocenylenedimethylsilylene), PFDMS, indicate a 3D crystalline phase with monoclinic packing of the macromolecules with possible unit cell parameters a = 13.29 Å, b = 6.01 Å, c = 13.9 Å, and γ = 93.6°. There are two main chains with four monomer units per unit cell, X-ray crystal density ρ_c = 1.455 g cm^{-3}, possessing a planar all-trans zigzag conformation of the main chain, helix 2/1. Poly(ferrocenylenedibutylsilylene), PFDBS, also appears to crystallize in a monoclinic lattice with unit cell parameters a = 11.57 Å, b = 6.71 Å, c = 13.6 Å and γ = 107.1° (two monomer units of one macromolecule per unit cell; X- ray crystal density ρ_c = 1.239 g cm^{-3}). A particular feature of crystalline PFDMS, and PFDBS, is the coexistence of the 3D monoclinic crystalline phases with mesophases (2D crystals with a hexagonal or tetragonal packing of macromolecules). Upon doping with iodine vapor, the crystalline poly(ferrocenylenedimethylsilylene) converts into a crystalline mixed-valence complex. Doped oriented samples retain the initial orientation of the macromolecules and also give relatively good fiber diffraction patterns. Equatorial reflections on such fiber patterns can be indexed by a 2D monoclinic packing of the complex macromolecules in the (*ab*) plane with unit cell parameters a = 10.36 Å, b = 6.03 Å, and γ = 90.7°. The values of the a and b dimensions suggest that $[I_3]^-$ species are placed between macromolecules and along their backbone. Three meridional reflections at 3.0, 4.0, and 6.0 Å yield a fiber repeat equal to 12.0 Å, which probably arises from a one-dimensional order of $[I_3]^-$ arrays.

Introduction

The study of inorganic/organometallic materials is developing rapidly in the hope that the metallic component can bring new and unusual properties to the resulting materials.[1] The longstanding interest in organometallic polymers containing ferrocene (Fc) groups is due to the thermal and photochemical stability of the Fc group and its well-established redox properties.[2] The incorporation of silicon groups with ferrocene substituents into polymeric materials has also been investigated.[3] The thermal and metal-catalyzed ring-opening polymerization (ROP) of [1]-silaferrocenophanes[4−10] has received considerable attention due to the potentially interesting properties of the resulting polyferrocenylene organosilylene materials (PFOS) containing a ferrocenylene group as an integral part of the polymer backbone, eq 1.

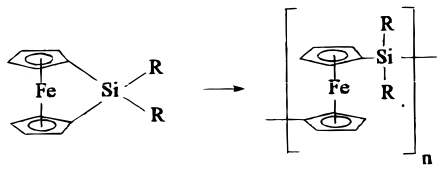

(1)

The main chain of PFOS consists of alternating ferrocene units and silane groups providing the possibility of a considerable electrostatic interactions between neighboring iron centers, especially in a charged state. Experimentally, this has been illustrated by the two-stage electrochemical oxidation of iron atoms in PFOS macromolecules.[4,5,8,10] Among other important characteristics reported for PFOS with various substituents R on silicon are their electroconductivity upon doping with iodine,[11] potential preceramic properties,[12] and variable refractive index properties.[8c]

The conformational behavior of PFOS with different substituents on silicon is of interest since conformational changes, which can also occur upon a partial oxidation of the ferrocenylene groups (for instance due to formation of charge-transfer salts with iodine[11] and tetracyanoethylene[13]) are likely to directly impact the polymer properties. Calculations of possible conformations of oligomeric ferrocenylenedimethylsilylenes, containing three, four, and five ferrocene units, both as isolated molecules and in the solid state, have been reported, including comparison with experimental X-ray crystalline structures.[14,15] The conformation of the macromolecules and their packing in the crystal form were proposed to be like that found for the pentamer.[10]

To date there has been no detailed report on X-ray diffraction data from the crystalline structure of high molecular weight PFOS. We now present X-ray diffraction data on the crystalline structures of high molecular weight poly(ferrocenylenedimethylsilylene) [PFDMS], its iodide complex and poly(ferrocenylenedibutylsilylene) [PFDBS].

Experimental Section

Poly(ferrocenylenedimethylsilylene) and poly(ferrocenylenedibutylsilylene) were synthesized by thermal polymerization of the corresponding [1]-silaferrocenophanes following the reported procedure.[5,8] Two poly(ferrocenylenedimethylsilylene) samples, i.e., PFDMS-A (M_w = 116 000 and M_w/M_n = 2.1) and a specially separated fraction PFDMS-B (M_w = 13 800 and M_w/M_n = 1.6), and a poly(ferrocenylenedibutylsilylene) sample (M_w = 71 000 and M_w/M_n = 1.9) were prepared. The molecular weight characteristics were measured by means of GPS in THF (polystyrene standards) using a Waters liquid chromatograph

10.1021/ma000343h CCC: $19.00
Published on Web 08/25/2000

equipped with a M600 pump, 2μ-Styragel linear columns, and M 484 UV−vis and M 410 refraction index detectors and provided with Maxima Software.

PFDMS and PFDBS films were cast from benzene solutions at ∼20 °C. Doping of PFDMS-A films with iodine was carried out by exposing them to iodine vapor at a pressure of $\sim 10^{-1}$ Torr for ∼1 h. The doped films were stabilized for 1−2 h and then exposed to high vacuum (not less than 4 h) to eliminate excess iodine. The amount of absorbed iodine was monitored by direct weighing, and we noted that the films gained up to 7 iodine atoms per iron atom. After pumping, the ratio I/Fe decreased to values of ∼3.2−1.4. The various iodine content data were also confirmed by direct elemental analysis.

Oriented films were obtained by means of the co-extrusion technique. The polymer film was placed between lead split rodlike billet halves and extruded at temperatures between 90 and 125 °C using dies with a conical entrance. By pulling the billet through the die, a reduction in its cross section area, and hence draw, was imposed. The attained nominal extension ratio of the film was ∼4.

DSC measurements were performed on a DSM-3 calorimeter (Pushino Biopribor, Russia) at heating rates of 8 and 16 °C/min using 10−20 mg samples. X-ray fiber photographs were recorded using flat-plate cameras (with specimen to film distances of 40−45 mm). X-ray diffractograms of nonoriented samples and oriented films at various angles to the orientation direction were obtained on a DRON-3 diffractometer (Russia) fitted with heater and temperature controlled within ±1°. Nickel-filtered Cu Kα radiation was used. Raman spectra were recorded with a Ramanor HG-2S laser spectrometer using 514.5 nm line from an ILA-120 argon laser. IR spectra were recorded by means of an IR Specord 82 on samples dispersed in Nujol on KBr plates. The density of the polymer films was determined by a flotation method in aqueous solution of $K_2[HgI_4]$.

Results and Discussion

Poly(ferrocenylenedimethylsilylene). PFDMS is a crystalline polymer with a melting point and heat of fusion varying in the range of 100−140 °C and 7.2−14.7 J g^{-1} respectively, depending on the MW and thermal history of the polymer sample.[16] A conspicuous feature of the published X-ray diffractograms of precipitated or solution-cast high molecular weight PFDMS samples is the existence of only one well-defined intense reflection at 6.34 Å.[8a] In contrast, the X-ray diffractogram of a melt-crystallized PFDMS sample, of low MW and narrow MWD, exhibits two sharp reflections at 6.65 and 6.02 Å.[16]

We have found that the melting point and heat of fusion also depend on the method of sample preparation (precipitation, solution casting, solvent used) and employed benzene cast films of PFDMS-A previously annealed at 125 °C in order to achieve a higher degree of crystallinity. The DSC trace for such a nonoriented sample is presented in Figure 1 (curve a). This film melts at 137 °C (DSC peak temperature) with a heat of fusion of 9.2 J g^{-1}. Its X-ray diffractogram shown in Figure 2 (curve a) is practically similar to that published earlier.[8a] There is an intense reflection at 6.36 Å and several very weak reflections at diffraction angles between 10 and 30°.

Orientation of solution cast films of PFDMS-A by extrusion led to a widening of the melting temperature range and a shift of the melting peak on DSC traces to higher or lower temperatures depending on extrusion conditions (temperature, shear stress and extension ratio). DSC traces for specimens oriented at various temperatures are illustrated in Figure 1. A certain distortion and breaking of initially formed crystals, their reorganization, and the appearance of strained tied

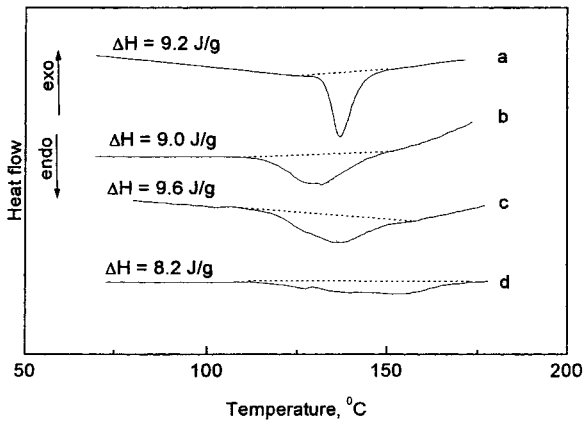

Figure 1. DSC traces for an original nonoriented PFDMS sample annealed at 125 °C for 30 min (a) and samples oriented at different temperatures: 100 °C (b), 115 °C (c), and 125 °C (d). Heating rate = 16 °C/min; ΔH is the heat of fusion of the sample.

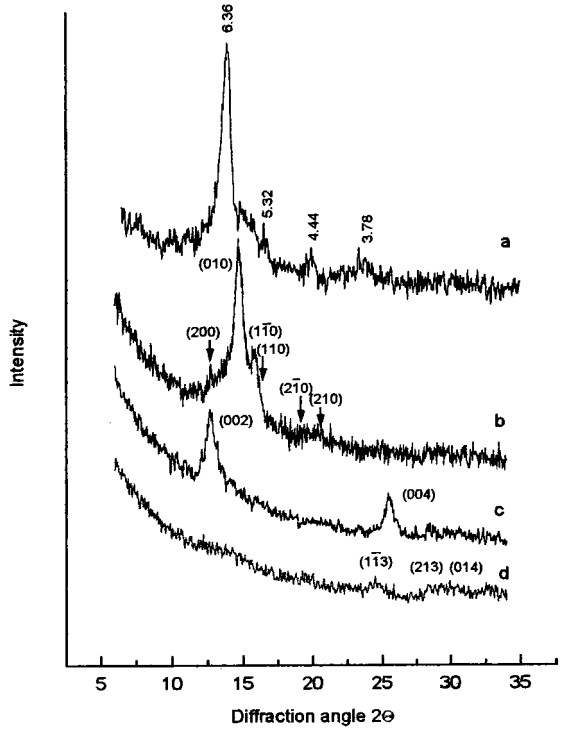

Figure 2. X-ray diffractograms of a nonoriented PFDMS film (a) and an oriented film, scanned along the equator (b), along the meridian (c), and at an angle of 55° to the equator on the X-ray fiber pattern (d) (see Figure 3). Data shown are *d* spacings (Å) and (*hkl*) indices (Table 1).

macromolecules may be reasons for the observed changes in the DSC traces. The maximum melting peak temperature that we attained was ∼150 °C (Figure 1, curve d), this being higher than the proposed equilibrium melting temperature for PFDMS (143 °C[16]) but close to the melting point of the ferrocenylenedimethylsilylene oligomer containing five ferrocene units (152 °C[10]). Orientation did not result in any appreciable change in the heat of fusion, ∼ 9 J g^{-1}.

Informative X-ray fiber patterns were obtained from oriented films of PFDMS-A. Such a pattern and its schematic drawing are shown in Figure 3. In all, 11 reflections positioned on the equator, the meridian and three layer lines can be distinguished; all the off-meridional reflections are very weak. The X-ray diffractograms taken along the equator, along the meridian,

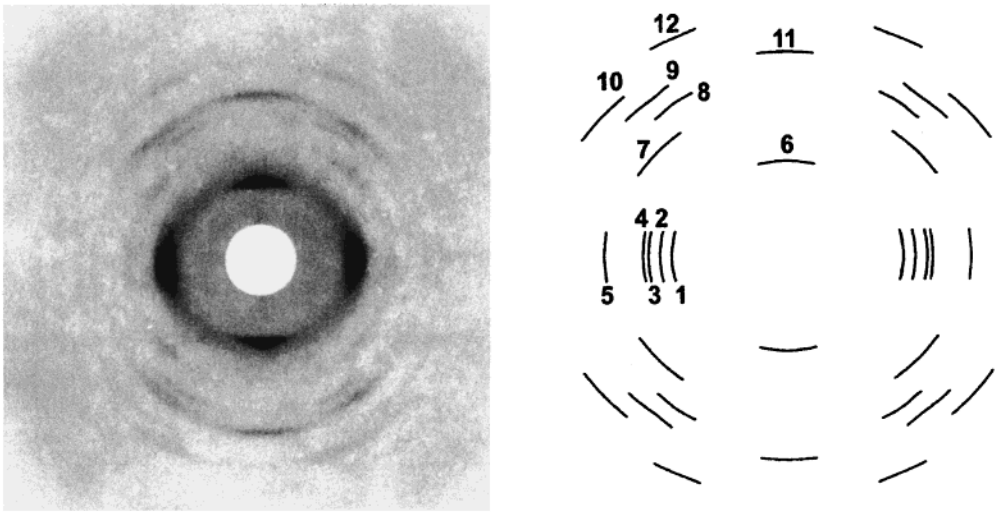

Figure 3. X-ray fiber pattern and its schematic drawing for an oriented PFDMS film.

and at an angle of 55° to the equator in the X-ray fiber pattern are presented in Figure 2. Surprisingly, the most intense, sharp reflection at 6.36 Å, observed in X-ray diffractograms of the initial isotropic films, was found to disappear completely upon orientation, and all the reflections recorded in the X-ray fiber patterns correspond to the weak ones of the isotropic specimen.

There are three clear-cut reflections on the equator at 5.60 Å ($2\theta = 15.83°$), 6.0 Å ($2\theta = 14.76°$), and 6.63 Å ($2\theta = 13.36°$). The first two and most intense are manifested in the diffractogram of the initial isotropic specimen as the right shoulder of the very strong reflection at 6.36 Å. The third reflection at 6.63 Å is weak, and its sharpness and intensity depend on orientation conditions. We could detect it as a separate well-defined reflection in fiber patterns taken from specimens oriented at 120 °C using larger specimen-film distances in the X-ray camera. The reflection at 5.32 Å, clearly displayed in the X-ray pattern of the nonoriented specimen, appears to transform upon orientation into the right-hand shoulder of the reflection at 5.60 Å (cf. curves a and b in Figure 2). All reflections are superimposed on a rather broad halo centered at ~14° in 2θ. This halo seems to be formed by the degeneration of the intense reflection at 6.36 Å upon orientation. The diffracted intensity of this amorphous-like peak is concentrated in the equator as deduced by comparing the diffractograms in Figure 2 taken along the equator and at an angle of 55° to the equator (curves b and d). On the equator of the fiber pattern there is also a very weak diffuse reflection in the vicinity of $2\theta \approx 20°$ (see also curve *b* in Figure 2).

The four equatorial reflections at 6.63, 6.00, 5.60, and 5.32 Å are in principle consistent with a monoclinic packing of PFDMS macromolecules in the (*ab*) crystallographic plane with unit cell parameters $a = 13.29$ Å, $b = 6.01$ Å and $\gamma = 93.6°$ and can presumably be indexed as (200), (010), ($1\bar{1}0$) and (110). In this case the occurrence of the small broad equatorial peak at 20° in 2θ can be regarded as a result of overlapping weak ($2\bar{1}0$) and (210) reflections at 19.3 and 20.6° in 2θ from the crystal lattice slightly distorted upon orientation. These conclusions are based on the small number of the equatorial reflections; thus, another unit cell cannot be excluded.

Two meridional reflections at 6.95 and 3.48 Å correspond to the second and fourth order of the 13.9 Å fiber repeat. The weak off-meridional reflections, located consequently on the second, third and fourth layer lines, are also consistent with this periodicity along the *c*-axis in the monoclinic lattice with the *a*, *b*, and γ parameters noted above. The list of all the reflections and their indices, the observed and calculated *d* spacings are given in Table 1. According to the published calculations,[14,15] the 13.9 Å periodicity along the macromolecular axis should correspond to the length of two monomer units in the planar all-trans zigzag conformation of the main chain (helix 2/1) schematically depicted in Figure 4.

Thus, the oriented PFDMS specimens appear to contain only one ordered phase, i.e., the monoclinic crystalline phase, I ($a = 13.29$ Å, $b = 6.01$ Å, c = 13.9 Å, and $\gamma = 93.6°$) containing two main chains with four monomer units per unit cell). The calculated crystal density ρ_c of this phase is 1.455 g cm^{-3} (data on the

Table 1. Miller Indices, *d*-Spacings, and Eye-Estimated Intensities of the Reflections for Oriented Phase I of PFDMS

N^a	*hkl*	d_{calcd} (Å)	d_{expt} (Å)	intensity[c]
1	200	6.63	6.63	w
2	010	6.0	6.0	s
3	$1\bar{1}0$	5.60	5.60	w
4	110	5.34	5.32[b]	w
5	$2\bar{1}0$	4.32	4.43	vw
	$2\bar{1}0$	4.59		
6	002	6.95	6.94	m
7	012	4.54	4.54	vw
8	$20\bar{3}$	3.80	3.81	vw
9	$1\bar{1}3$	3.57	3.57	vw
10	213	3.16	3.14	vw
11	004	3.47	3.48	w
12	014	3.01	3.0	w

[a] Number of reflections indicated in Figure 3. [b] *d* spacing taken from the diffractogram *a* in Figure 2. [c] s = strong, m = medium, w = weak, and vw = very weak.

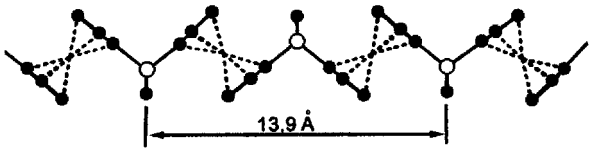

Figure 4. Schematic presentation of all-trans conformation of PFDMS macromolecule. Open and solid circles are silicon and carbon atoms, respectively. Periodicity along the macromolecule axis is 13.9 Å.

experimentally determined density are presented below). It seems that this phase is the same one observed previously in studies on the melt-crystallized low molecular weight PFDMS[16] as the latter exibits two quite intense X-ray diffraction reflections at 6.65 and 6.02 Å.

On the other hand, along with phase I, nonoriented films of PFDMS-A contain an extra ordered phase (phase II) as deduced from the existence of the very intense reflection at 6.36 Å in their X-ray diffractograms. The remainder of the reflections in these diffractograms can in principle be assigned to phase I (see Figure 2 and Table 1). It is difficult to say unambiguously whether there are other reflections related to phase II. The intensities of the diffraction peaks in the vicinity of 20° and 23.4° in 2θ ($d = 4.44$ and 3.78 Å) are too strong to be attributed only to the $(2\bar{1}0)$, (210) and (012) and (203) reflections of phase I, since, as noted from the X-ray fiber pattern (Figure 3) and the diffractograms b and d in Figure 2, these reflections, which are positioned in the vicinity of the same diffraction angles, are very weak. Furthermore, the ratios of the d spacing values $6.36/4.44 \cong 1.43$ and $6.36/3.78 \cong 1.68$ are very close to $\sqrt{2}$ and $\sqrt{3}$, and hence, the reflections at 4.44 and 3.78 Å may also be associated with phase II, suggesting a packing of PFDMS macromolecules close to tetragonal and/or hexagonal.

We found no other reflections that could be attributed to this phase. Consequently, phase II can be regarded as a partially ordered phase (mesophase) apparently formed by conformationally disordered macromolecules. In this regard, it is noteworthy that a single intense and sharp interchain reflection is a characteristic feature of X-ray diffractograms of various mesomorphic polysiloxanes, polysilanes, and polyphosphazenes. According to the theoretical calculations on the structure of ferrocenylenedimethylsilylene oligomers,[14,15] there exist a number of conformers with energies close to the deepest conformational energy minimum and this fact can be one reason for the formation of such a partially ordered phase. The orientation procedure leads to the complete disappearance of phase II, but leaves the heat of fusion practically unchanged, therefore it seems that the 3D crystalline phase I is mainly responsible for the observed total heat of fusion.

The crystalline phase I and mesophase II, which coexist in the nonoriented high molecular weight PFDMS-A samples, do not interconvert upon heating and melt in the same temperature range, corresponding to the melting peak on the DSC traces. This is illustrated in Figure 5 where X-ray diffractograms of nonoriented and oriented specimens, taken at different temperatures, are presented. The amorphous halo, developed in the course of melting, is centered at ~13.1° in 2θ at 160 °C and its center shifts to ~13.5 in 2θ after cooling to ambient temperature. Neither isotropic nor oriented specimens were found to crystallize on cooling. The density of the cooled amorphous PFDMS-A sample was measured to be $\rho_a = 1.294$ g cm^{-3}.

Both the precipitated and benzene cast samples of the low molecular weight PFDMS-B contained both phases I and II. However, they melted with higher heats of fusion (~13.5 J g^{-1}, close to the maximum value of 14.7 J g^{-1} reported for PFDMS[16]). The DSC traces of such a sample, shown in Figure 6, exhibit a multiple melting peak whose profile, position and overall area depend on the sample thermal history. Annealing at temperatures from 105 to 110 °C led only to redistribution of the area

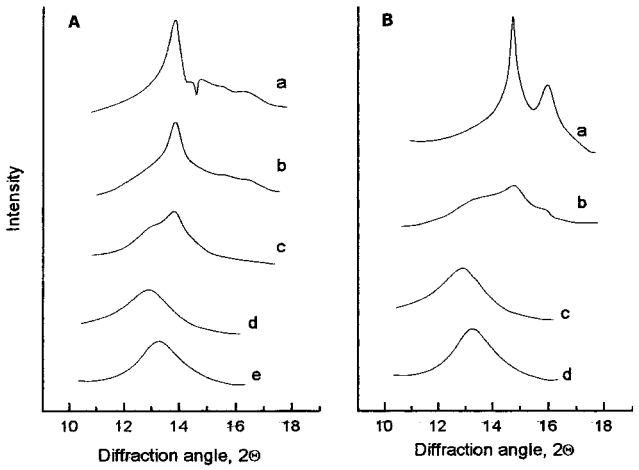

Figure 5. X-ray diffractogram of a nonoriented sample (A) and equatorial X-ray diffractogram of an oriented film (B) taken at different temperatures. Key for A: ambient temperature (a); 110 °C (b); 130 °C (c); 160 °C (d); cooled to ambient temperature (e). Key for B: ambient temperature (a); 130 °C; (b) 160 °C (c); cooled to ambient temperature (d).

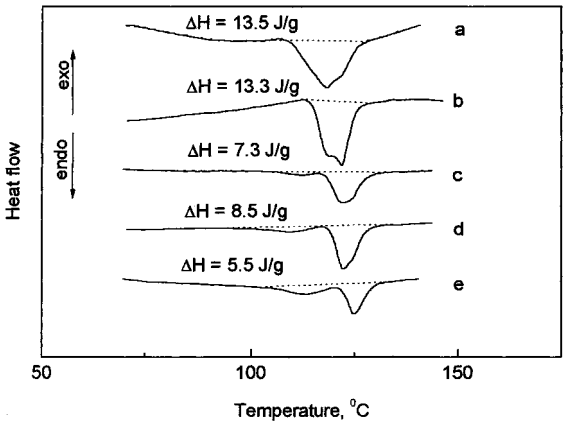

Figure 6. DSC traces for a low molecular weight PFDMS-B sample annealed at 105 (a), 110 (b), 112 (c), 115 (d), and 118 °C (e). Heating rate = 8 °C/min; ΔH is the heat of fusion of the sample.

under the overlapping peaks at 118 and 122 °C with no change in overall value. At higher annealing temperatures the maximum at 118 °C degenerated into a shoulder and then disappeared, replaced by a peak at 125 °C and a third small, rather broad peak centered at about 110 °C. Simultaneously the overall heat of fusion decreased considerably (see Figure 6). These facts suggest that, upon annealing, initially formed crystals reorganized into larger and/or more perfect ones, but concurrently, some of them melted giving rise to formation of even smaller crystals upon subsequent cooling. It is noteworthy that the increase in the long-period, measured by small-angle X-ray scattering, for the PFDMS sample of approximately similar MW, starts with a crystallization temperature of ~110 °C.[16]

X-ray diffractograms of the annealed PFDMS-B samples display neither a new phase nor the disappearance of phases I and II (see Figure 7). A noticeable difference in the X-ray diffractograms of samples annealed at temperatures above 112 °C is the appearance of the left-hand shoulder of the 6.36 Å reflection, which is centered at ~13.5° in 2θ and reflects an increase in the amorphous phase content. This finding is in line with the decrease in the heat of fusion noted above.

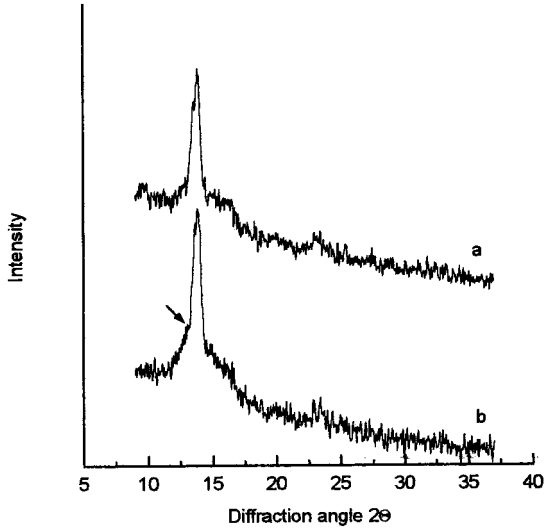

Figure 7. X-ray powder diffractograms of a low molecular weight PFDMS-B sample annealed at 105 (a) and 115 °C (b). The arrow points to the amorphous halo.

Thus, the concurrent formation of phases I and II appears to be an intrinsic feature for the crystallization of different molecular weight PFDMS from solution in the course of precipitation or solvent evaporation. Phase I is the 3D-crystalline phase, whereas phase II is a 2D-crystalline mesophase. The main X-ray diffraction characteristic of the latter is the intense, sharp interchain mesomorphic reflection at 6.36 Å, which earlier was tentatively attributed to a 3D-crystalline phase.

Both phases melt simultaneously with the main input into the heat of fusion coming from phase I. Therefore, we propose that the mesophase domains are locked by phase I crystallites, or incorporated as rather large defect regions in phase I. Along with phases I and II, crystalline PFDMS samples contain an amorphous phase. The amorphous content is not high judging from the intensities of the amorphous halo in the X-ray diffractograms of the isotropic and oriented specimens shown in Figure 2 (curves a and d).

According to the measured heats of fusion, the content of phase I in PFDMS samples can vary in a wide range depending on molecular weight, preparation conditions of the sample, and its thermal history. Corresponding changes in density are also expected. Indeed, the densities of three benzene cast films with the measured heats of fusion equal to 13.5, 8.2, and 5.0 J g^{-1} were found to be 1.374, 1.341, and 1.318 g cm^{-3} respectively. Assuming that the heat of fusion of mesophase II can be neglected to a first approximation, a tentative linear extrapolation of these values to r_c for phase I (1.45 g cm^{-1}) permits a rough estimate for the heat of fusion of the neat crystalline phase of ~26 J g^{-1}, which may be regarded as a limiting high value.

Poly(ferrocenylenedibutylsilylene). PFDBS is also a crystalline polymer which melts at 120−140 °C.[8a] Our DSC measurements have shown that as-cast PFDBS samples exhibit a double melting peak with maxima at 132 and 139 °C (see trace a in Figure 8). In contrast to PFDMS, PFDBS crystallize easily from the melt in cooling runs (trace d). After the sample is annealed at 120−140 °C, the first maximum is shifted slightly to higher temperatures and its proportion diminishes. Simultaneously the heat of fusion increased from 9.4 to 14.8 J g^{-1}. Subsequent annealing at 135 °C resulted in the occurrence of only one melting peak at 141 °C

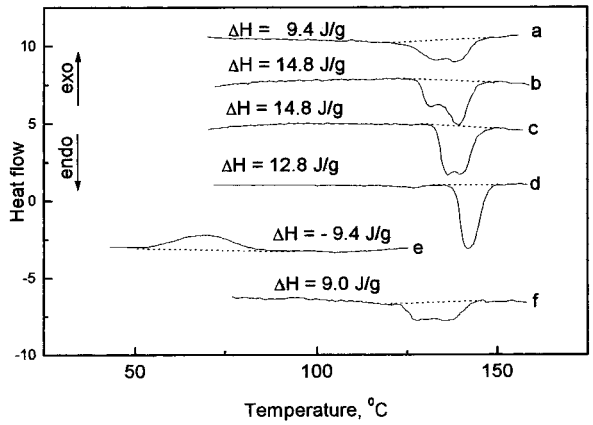

Figure 8. DSC traces for PFDBS upon heating (a, b, c, d, and f) and cooling (e): original sample (a); samples annealed at 125 (b), 130 (c), and 135 °C (d); sample oriented at 120 °C (f). Heating/cooling rate = 16 °C/min; ΔH is the heat of fusion of the sample.

and a small decrease in the heat of fusion to 12.8 J g^{-1}. Such thermal behavior points to reorganization, perfection, and partial melting of the initially formed crystals.

X-ray diffraction patterns of both initial and annealed nonoriented PFDBS specimens display many diffraction rings (Figure 9) which correspond entirely to the reflections seen in the X-ray powder diffractogram of the high molecular weight polymer,[8a] reproduced for comparison in Figure 10. Orientation of benzene cast films by extrusion had little affect upon the heat of fusion and melting temperature (compare DSC traces a and f in Figure 8).

We were unable to achieve the same degree of orientation for PFDBS as with PFDMS. The X-ray diffraction pattern of an oriented specimen, Figure 9, does not contain well-defined oriented reflections, and only a limited concentration of diffraction intensity in the equator (arcing) for four reflections with *d*-spacing 11.06, 6.41, 5.54, and 4.95 Å can be observed. Consequently, these reflections were attributed to equatorial ones and the others, which undoubtedly are not arced on the equator, were regarded as off-equatorial. Despite the scarcity, these X-ray diffraction data proved to be enough for tentative lattice constants of PFDBS crystal to be evaluated. The equatorial reflections are consistent with a monoclinic packing of the macromolecules with possible unit cell parameters $a = 11.57$ Å, $b = 6.71$ Å and $\gamma = 107.1°$, being indexed as (100) ($d = 11.06$ Å), (010) and ($1\bar{1}0$) ($d = 6.41$ Å), (200) ($d = 5.54$ Å), and (110) ($d = 4.95$ Å). The other reflections observed in the X-ray diffractogram patterns (Figures 9 and 10) can be identified as (001) ($d \cong 13.6$ Å), (101) ($d \cong 8.6$ Å), and (111) and/or (012) ($d = 4.67$ Å) with an average fiber repeat of 13.6 Å. Two other very weak peaks in the X-ray diffractograms at $2\theta \cong 15.3°$ ($d = 5.79$ Å) and $2\theta \cong 24.2°$ ($d = 3.67$ Å) fit the above periodicity along the *c* axis and can be indexed as (011) and (013), respectively. A unit cell with the above parameters should contain two monomer units of one macromolecule and have X-ray crystal density equal to 1.239 g cm^{-3}. The density of a sample with the heat of fusion equal to 9.0 J g^{-1} was found to be 1.172 g cm^{-3}.

Two peculiar features of the X-ray diffraction patterns are noteworthy. The first is the absence of an appreciable amorphous halo that implies a rather low content of completely disordered phase in the samples. The second is that the ratio of *d* spacings at 11.06 and

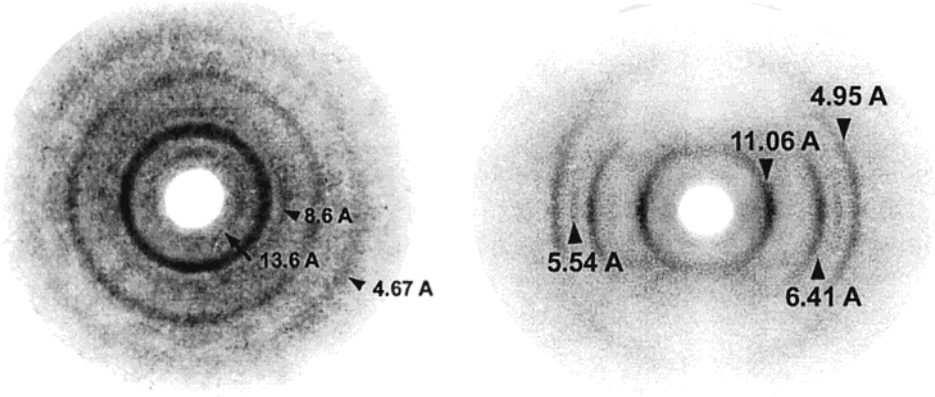

Figure 9. X-ray diffraction patterns for nonoriented (left) and oriented (right) PFDBS films.

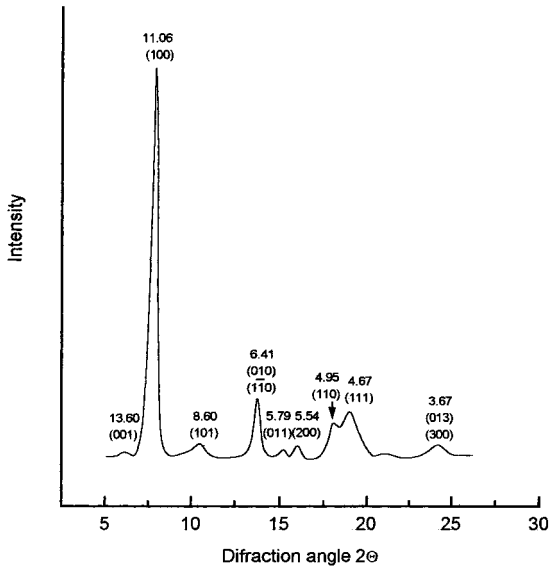

Figure 10. X-ray diffractogram of a nonoriented benzene cast film of PFDBS Reprinted from ref 8a. Copyright 1993 American Chemical Society. Data near the peaks are *d* spacing (Å) and (*hkl*) indices.

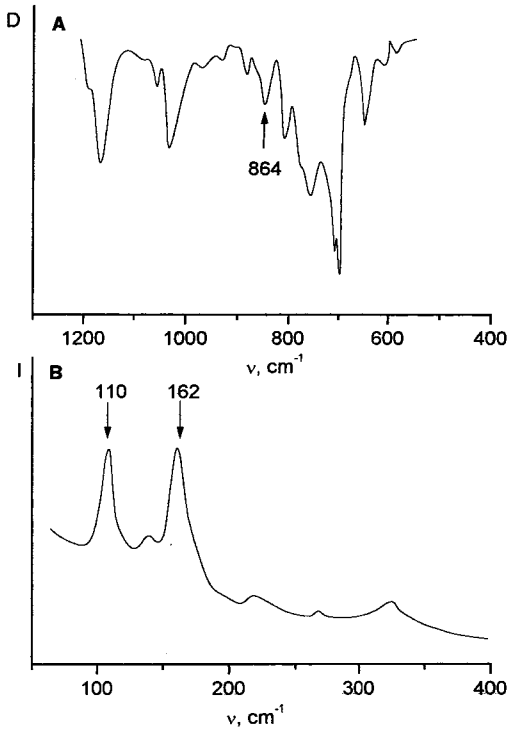

Figure 11. IR (A) and Raman (B) spectra of iodide complex of PFDMS with the atomic ratio I/Fe = 3.2.

6.41 Å is almost exactly $\sqrt{3}$, indicating a possible hexagonal packing of the macromolecules. Coupling this observation with the very high intensity and sharpness of the interchain reflection (usually observed for various mesomorphic polymers) we suggest that crystalline PFDBS samples, as with their PFDMS analogues, may coexist as two ordered phases: a 3D monoclinic phase and a 2D hexagonal crystalline phase (mesophase) characterized by the 11.06 Å interchain *d* spacing and reflection at 6.41 Å.

Iodide Complex of Poly(ferrocenylenedimethylsilylene). By analogy with the well-known iodide complexes of low molecular weight organic compounds,[17] iodide complexes of PFDMS are low-dimensional solids whose structure, in terms of the type of polyiodide anions $I^-{\cdot}nI_2$ and their mutual packing with oxidized molecules, is a key factor in the understanding of their electrical properties. We have investigated the structure of isotropic and oriented PFDMS films doped with various amounts of iodine (the atom ratio I/Fe = 1.4−3.2) and found that all these materials are crystalline. Iodine doping leads to the formation of mixed-valence macromolecules in which ferrocene moieties alternate with ferrocenium species possessing I_3^- and I_5^- as counteranions in different proportions depending on the overall iodine content.[20] The characterization of the doped polymer involved the use of IR and Raman spectroscopy. According to the IR spectrum of a doped film with the ratio I/Fe = 3.2 (Figure 11 A), only about 40% of monomer units are converted into oxidized ferrocenium ions. This rough assessment was made on the basis of the intensity of the band at 864 cm^{-1} which is ascribed to the perpendicular cyclopentadienyl C−H bend in ferrocenium ion.[18,19] As an internal reference we used the band at 1037 cm^{-1} whose intensity was found to change only slightly upon the complete oxidation of ferrocene moieties.[20,21] The Raman spectrum of this doped film, Figure 11B, contains two peaks of approximately equal intensities at 110 and 162 cm^{-1}, which are related to the stretching mode of vibration in linear I^-_3 and I^-_5 species.[17]

These facts imply that the doped film can be heterogeneous and contain domains with various iodine content and polyiodide anions of at least two types. Upon prolonged pumping, the iodine content in the doped films is lowered and concurrently the intensity of the

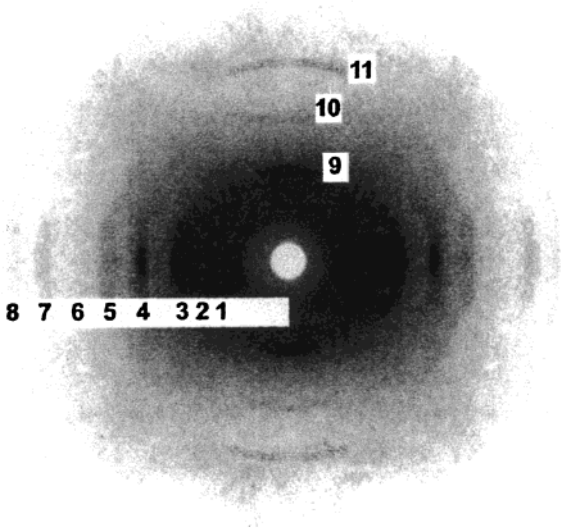

Figure 12. X-ray diffraction pattern of an oriented film of PFDMS.iodide complex. Figures near the reflections are their numbers in Table 2.

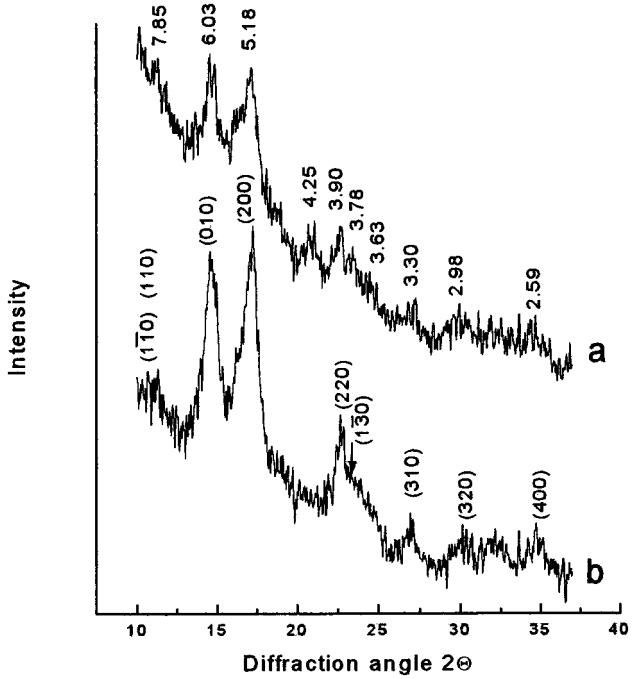

Figure 13. X-ray powder diffractograms of PFDMS.iodide complexes with the atomic I/Fe ratio equal to 3.2 (a) and 2.5 (b). Data near the peaks are *d* spacing (Å) and (*hkl*) indices of equatorial reflections. The intensities are not normalized to the sample thickness.

band at 162 cm^{-1} decreases. With the ratio I/Fe = 1.4, I_3^- species predominate. However, irrespective of the iodine content all the doped PFDMS films displayed similar X-ray diffraction patterns revealing a common crystalline phase involving mixed-valence macromolecules in which ferrocene moieties alternate with ferrocenium ions having supposedly I^-_3 as counteranions.

Oriented films doped with iodine gave fair fiber X-ray patterns. A characteristic feature of all the fiber patterns is the location of at least seven reflections at 6.03, 5.18, 3.93, 3.30, 2.98, 2.59, and 2.35 Å on the equator, six of which we also observed in X-ray diffractograms of doped isotropic films (see Figures 12 and 13). At sufficiently long X-ray exposure time the fiber X-ray diffraction patterns exhibit a weak equatorial reflection

Table 2. Miller Indices and *d*-Spacings of Equatorial Reflections for the Iodide Complex of PFDMS

N^a	(*hkl*)	d_{calcd} (Å)	d_{expt} (Å)
1	1$\bar{1}$0	7.92	7.85
	110	7.80	
2	010	6.03	6.03
3	200	5.18	5.18
4	2$\bar{2}$0	3.90	3.90
4a[b]	1$\bar{3}$0	3.78	3.78
5	310	3.31	3.30
6	320	2.98	2.98
7	400	2.59	2.59
8	1$\bar{5}$0	2.34	2.35
	150	2.36	

[a] Number of reflection indicated in Figure 12. [b] *d*-spacing taken from the X-ray diffractogram in Figure 13.

at ∼7.85 Å, which is in principle consistent with a monoclinic packing of the macromolecules in the (*ab*) plane with unit cell parameters $a = 10.36$ Å, $b = 12.06$ Å, and $\gamma = 90.9°$. The proposed indices of these reflections are indicated near the corresponding peaks in Figure 13 and listed in Table 2. Two weak reflections at 6.0 and 2.98 Å and a very weak third one at ∼4 Å (for specimens properly tilted toward the X- ray beam) could be distinguished on the meridian of the fiber patterns (reflections 9, 10, and 11 in Figure 12, respectively). These meridional reflections can presumably be identified as the second, third, and fourth orders of a fiber repeat of 12 Å.

Three features of the crystalline iodide material formation are noteworthy:

a. Doping amorphous PFDMS films, prepared by cooling from the melt (see above), yields amorphous iodide complexes.

b. Doping both nonoriented films of the pristine PFDMS, containing the crystalline phase I and the mesophase, and oriented films containing only phase I result in the same crystalline phase.

These facts imply that the formation of the crystalline complex proceeds as a topochemical reaction involving at least phase I.

Introduction of iodine molecules into the crystal lattice of PFDMS leads to the ∼4 Å increase in the separation of the macromolecules in the complex crystal. The observed value of $a = 10.36$ Å is in good agreement with one oxidized macromolecule in the unit cell and the location of I_3^- anions between the macromolecules. Taking into account the lateral dimension of the PFDMS macromolecule itself along the *a* axis (half the *a* parameter of the PFDMS crystal unit cell = 6.65 Å), the distance between the iron and iodine atoms in ferrocenium triiodide (4.92 Å[22]) and the van der Waals radius of iodine atom (2.15 Å), the periodicity along the *a* axis in the complex crystal is expected to be (6.65/2 + 4.92 + 2.15) = 10.39 Å. Since parameters *b* and γ of the complex crystal changed very little (6.03 vs 6.0 Å and 90.7 vs 93.6°), it seems that the rodlike triiodide anions should lie along the macromolecule axes.

The periodicity along the backbone of the iodinated macromolecules is shorter by about 2 Å than that in the pristine polymer crystal. This reflects a distortion of the all-trans conformation of the main chain, which is apparently caused by changes in inter- and intramolecular interactions of the oxidized macromolecules containing the charged iron centers with the polyiodide counteranions. The presence of only weak meridional reflections on the layer lines may imply that the oxidized macromolecules themselves are conformation-

ally disordered and the meridional reflections are related to one-dimensional order in an arrangement of I_3^- anions. Note that the length of I_3^- anion is ~9.7 Å, which consequently falls in the observed fiber repeat, in contrast to the linear I_5^- anion whose length is ~15.5 Å.[23]

In the X-ray diffractograms of the doped samples with large iodine content (I/Fe > 3), two additional reflections can be observed at 3.63 and 4.25 Å (see Figure 13, curve a) which are oriented on the equator in the corresponding fiber patterns. These reflections are not consistent with the unit cell parameters above and represent another ordered phase formed by the iodinated macromolecules or an ordered arrangement of various polyiodide anions $I^-{\cdot}nI_2$ in noncrystalline regions.

Conclusions

On the basis of the X-ray diffraction patterns of nonoriented and oriented samples of PFDMS and PFDBS, we have inferred that crystalline PFDMS, and probably PFDBS, involves the coexistence of 3D crystalline phases (monoclinic) and mesophases (2D crystals with a hexagonal or tetragonal packing of macromolecules). We suggest that the existence of the partially disordered crystalline phases is related to the close energies of the various conformations as determined by calculations of a series of oligomeric molecules. In the proposed 3D monoclinic phase PFDMS macromolecules possess the planar 2/1 helix conformation,[24] which was assumed earlier by analogy with the conformation of the central part of a ferrocenyleneorganosilane pentamer determined by X-ray crystallography.[10]

From the unit cell parameters for PFDMS the cross sectional dimensions of the PFDMS macromolecule, (a/2 = 6.65 Å and b = 6.01 Å), correlate well with two transverse dimensions of the isolated macromolecule possessing the planar zigzag conformation. In view of the monoclinic angle γ close to 90°, we propose that the planar zigzag main chain lies in the (bc) plane or slightly tilted to it, and consequently, the crystallographic arrangement of Si−C bonds is parallel (or close to parallel) to the (ac) plane. Lengthening the substituents on silicon in PFOS, Me to *n*-Bu, leads to an increase in the macromolecule dimension along the a axis by ~5 Å instead of the 7.6 Å expected for the all trans conformation of the butyl groups arranged parallel to the (ac) plane. This is accompanied by an increase in the macromolecule dimension along the b axis (0.72 Å), by a change in the monoclinic angle γ to 107° and by a decrease in the c dimension from 13.9 to 13.6 Å. Such dimensions suggest a skewed conformation of the butyl groups and a certain distortion of the all trans conformation of the main chains. A more detailed description of the packing of the macromolecules in PFDMS and PFDBS crystals can be gained only by means of a rigorous comparison of the observed and calculated reflection intensities.

A crystalline iodide complex of PFDMS was formed by the interaction of iodine vapor with the crystalline phases of the polymer. IR and Raman spectra and the crystal unit cell dimensions suggest a mixed-valence structure of the oxidized macromolecules having I_3^- species as counteranions. The complex crystal is undoubtedly characterized by the regular packing of macromolecules in the (ab) plane, but the conformation of the main chain is not clear.

Acknowledgment. This research was supported by the Civilian Research Development Fund (CRDF) for collaborative research between the USA and former Soviet Union countries (Grant No. RC1-278) and the Welch Foundation, Houston, TX (Grant No. AH-0546). We wish to thank Dr. L. A. Leites and Dr. S. S. Bukalov for IR and Raman spectra.

References and Notes

(1) (a) Zeldin, M.; Wynne, K. J.; Allcock, H. R. *Inorganic and Organometallic Polymers*; ACS Symposium Series 360; American Chemical Society: Washington, DC, 1988. (b) Mark, J. E.; Allcock, H. R.; West, R. *Inorganic Polymers*; Prentice Hall Polymer Science and Engineering Series; Prentice Hall: Englewood Cliffs, NJ, 1992.

(2) (a) Togni, A.; Hayashi, Eds. T. *Ferrocenes*; VCH: Weinheim, Germany, 1995. (b) Gonsalves, K. E.; Rausch, M. D. Chapter 36 in ref 1a. (c) Hayes, G. F.; George, M. H. In *Organometallic Polymers*; Carraher, C. E., Sheats, J. E., Pittman, C. U., Eds.; Academic Press: New York, 1978; p 13.

(3) (a) Zuaodung, D.; Xiaoyao, W.; Jing, L. *J. Shandong Univ.* **1987**, *115*, 22 (b) Pannell, K. H.; Rozell, J. M.; Zeigler, J. M. *Macromolecules* **1988**, *21*, 278. (c) Pannell, K. H.; Rozell, J. M.; Vincenti, S In *Silicon Based Polymer Science: A Comprehensive Resource*; Zeigler, J. M., Fearon, F. W. G., Eds.; Advances in Chemistry 224; American Chemical Society: Washington, DC, 1990; Chapter 20. (d) Diaz, A.; Seymour, M.; Pannell, K. H.; Rozell, J. M. *J. Electrochem. Soc.* **1990**, *137*, 503.

(4) Foucher, D. A.; Tang, B.-Z.; Manners, I. *J. Am. Chem. Soc.* **1992**, *114*, 6246.

(5) Nguyen, M. T.; Diaz, A. F.; Dementiev, V. V.; Sharma, H.; Pannell, K. H. *SPIE Proc.* **1993**, *1910*, 230.

(6) (a) Rulkens, R.; Ni, Y.; Manners, I. *J. Am. Chem. Soc.* **1994**, *116*, 12121. (b) Rulkens, R.; Lough, J. K.; Manners, I. *J. Am. Chem. Soc.* **1994,** *116*, 797.

(7) (a) Ni, Y.; Rulkens, R.; Pudelski, J. K.; Manners, I. *Macromol. Rapid Commun.* **1995**, *16*, 637. (b) Gomez-Elipe, P.; Macdonald, J.; Manners, I. *Angew. Chem., Int. Ed. Engl.* **1997**, *36*, 762.

(8) (a) Nguyen, M. T.; Diaz; A. F.; Dementiev, V. V.; Pannell, K. H. *Chem. Mater.* **1993**, *5*, 1389. (b) Nguyen, M. T.; Diaz, A. F.; Dementiev, V. V.; Pannell, K. H.; *Chem. Mater.* **1994**, *6*, 952. (c) Pannell, K. H.; Robillard, J. U.S. Patent No. 5,472,-786, 12/5/1995.

(9) (a) Foucher, D. A.; Ziembinski, R.; Tang, B.-Z.; Macdonald, P. M.; Massey, J.; Manners, I. *Macromolecules* **1993**, *26*, 2878. (b) Foucher, D. A.; Petersen, R.; Pudelski, J. K.; Edwards, M.; Ni, Y.; Massey, J.; Jaeger, R.; Vansco, G. J.; Manners, I. *Macromolecules* **1994**, *27*, 3992. (c) Pudelski, J. K.; Rulkens, R.; Foucher, D. A.; Lough, A. J.; Macdonald, P. M.; Manners, I. *Macromolecules* **1995**, *28*, 7301.

(10) Rulkens, R.; Lough, A. J.; Lovelace, S. R.; Grant, C.; Geiger, W. E. *J. Am. Chem. Soc.* **1996**, *118*, 12683.

(11) (a) Tanaka, M.; Hayshi, T. *Bull. Chem. Soc. Jpn.* **1993**, *66*, 334. (b) Manners, I.; *Adv. Organomet. Chem.* **1995**, *16*, 637. (c) Rulkens, R.; Resendes, R.; Manners, I.; Murti, K.; Fossum, E.; Miller, P.; Matyjaszewski, K. *Macromolecules* **1997**, *30*, 8165.

(12) Tang, B.-Z.; Petersen, R.; Foucher, D. A.; Lough, A.; Coombs, N.; Sodhi, R.; Manners, I. *J. Chem. Soc., Chem. Commun.* **1993**, 523.

(13) Pudelski, J. K.; Foucher, D. A.; Honeyman, C. H.; Macdonald, P. M.; Manners, I.; Barlow, S.; O'Hare, D. *Macromolecules* **1996**, *29*, 1894.

(14) Pannell, K. H.; Dementiev, V. V.; Li, H.; Cervantes-Lee, F.; Nguyen, M. T.; Diaz, A. F. *Organometallics* **1994**, *13*, 3644.

(15) Barlow, S.; Rohl, A. L.; Shi, S.; Freeman, C. M.; O'Hare, D. *J. Am. Chem. Soc.* **1996**, *118*, 7578.

(16) Lammertink, R. G. H.; Hempenius, M. A.; Manners, I.; Vansco, G. J. *Macromolecules* **1998**, *31*, 795.

(17) Marks, T. G.; Kalina, D. W. In *Extended Linear Chain Compounds*; Miller, J. S., Ed.; Plenum: New York, 1982; Vol. 11, p 197.

(18) Pavlik, I.; Klikorka, J. *Collect. Czech. Chem. Commun.* **1965**, *30*, 664.

(19) Duggan, D. M.; Hendrickson, D. N. *Inorg. Chem.* **1975**, *14*, 955. (b) Krammer, J. A.; Hendrickson, D. N. *Inorg. Chem.* **1980**, *19*, 3330.

(20) Bukalov, S. S.; Papkov, V. S.; Leites, L. A.; Espada, L.; Pannell, K. H. Presented at 32nd Organosilicon Symposium, Milwaukee, WI, March 1999; paper 65.
(21) According to the literature,[19] bands in the vicinity of ~813 and ~845 cm^{-1}, which are ascribed to an out-of-plane CH bending in ferrocene and ferrocenium ion respectively, can be used in analyzing the degree of oxidation in mixed-valence complexes of molecules containing two or more ferrocene centers. In the case of PFDMS, such an analysis is complicated due to the occurrence of torsional bands of $SiMe_2$ group in this frequency region. As a result the band at 819 cm^{-1} observed for the pristine PFDMS does not disappear upon doping with iodine, as should be expected for the complete oxidation of ferrocene moieties, but shifts to 828 cm^{-1}. The intensity of a band at 864 cm^{-1}, related to the CH bending in ferrocenium moieties of the completely oxidized iodide complex, was found to be higher by about an order of magnitude than that of a band at 867 cm^{-1} observed for the nonoxidized polymer.[20] The intensity of a band at 1037 cm^{-1}, related to an in-plane CH bending,[18] did not to change more than 10% upon doping and this band was chosen as a reference for a rough assessment of the degree of oxidation in the doped PFDMS.
(22) Bernstein, T.; Herbstein, F. H. *Acta Crystallogr.* **1968**, *B24*, 1640.
(23) Coppens, P. In *Extended Linear Chain Compounds*; Miller, J. S., Ed.; Plenum: New York, 1982, Vol. 1, p 333.
(24) X-ray fiber patterns of oriented films cast from solutions at temperatures below 15 °C often contain an additional meridional reflection at ~6.1 Å pointing to the existence an extra ordered phase with another conformation of the macromolecules. This question is under study, and corresponding results will be published separately.

MA000343H